DISTRIBUTION AND SPECIATION OF PHOSPHORUS IN FORESHORE SEDIMENTS OF THE THAMES ESTUARY, UK.

Andrew M Tye, Jeremy Rushton and Christopher H Vane*

British Geological Survey, Keyworth, Nottingham, NG12 5GG, UK.

*Author for correspondence (chv@bgs.ac.uk)

Abstract

Estuarine sediments can be a source of Phosphorus (P) to coastal waters contributing to nutrient budgets and geochemical cycles. Whilst salt marsh sediments have been extensively studied, fewer studies have examined the potential P storage of foreshore or inter-tidal mud flat deposits. In this work, the concentration and speciation of P in 47 cores were examined from the inter-tidal mud flats of the tidal river Thames, from west London to the North Sea (~120 km). Results of P concentration and speciation were combined with published data relating to known sediment dynamics and water chemistry within the estuary to produce a conceptual model of sediment-P behaviour. Highest concentrations of total P (median concentration ~3000 mg kg^{-1}) were found close to the centre of London, probably as a result of inputs from major sewage treatment works. However, results showed that significant P desorption occurred after sediment passed through the Estuarine Turbidity Maximum and when the salinity of the river water exceeded ~6 ppt. In the outer estuary median total P concentrations fell to ~1000 mg kg^{-1}. Organic and inorganic species of Phosphorus were extracted and it was found that organic P was desorbed to a greater extent than inorganic P in the lower estuary. Models were developed to predict Total P (R^2=0.80), oxalate extractable P (R^2=0.80) and inorganic P (R^2=0.76) from sediment geochemical and river water properties. As the foreshore mud flats consist of deposited suspended sediment, concentrations of inorganic and organic P reflect largely the effects water chemistry has on P speciation and concentration. Thus suspended sediment, along with remobilised sediment from the upper estuary are likely to undergo similar desorption processes as they pass down the estuary.

Keywords: Estuary, London, Phosphorus, Speciation

1. Introduction

51 The transport of phosphorus from terrestrial to oceanic environments has important
52 implications for the quality of fresh and marine waters (Eyre and Balls, 1999). The EU Water
53 Framework Directive (Directive EC 2000/60/EC) was introduced to prevent further
54 deterioration and improve the quality of inland surface waters whilst promoting 'good
55 ecological status' (GES) with respect to biodiversity in rivers (Johnes et al. 2007; EA, 2014).
56 In addition, the EU waste water Directive (Directive EU 91/271/EEC) aimed to reduce the
57 amount of P released from Sewage Treatment Works. However, whilst statutory legislation
58 for P concentrations in estuarine waters have yet to be introduced in the UK, improvements in
59 the quality of river water leaving the catchment are likely to impact estuarine and marine
60 systems as phosphorus is a key element contributing to eutrophication, algal and planktonic
61 blooms (Correll, 1998; Davidson et al. 2014).
62
63 Whilst aquatic P species may dominate the nutrient cycle within estuarine systems,
64 contributions to estuarine P budgets will also be derived from the P stored within the system,
65 including sediments. Thus an initial stage to understanding the contribution sediment-P
66 produces within estuarine waters is to obtain knowledge of the sediment distribution and
67 movement, along with changes in sediment-P speciation within the tidal length of the river
68 and estuarine system. The geology of the catchment controls important sediment properties
69 such as texture and geochemistry whilst the catchment geomorphology influences river
70 velocity and channel morphology which determines accumulation position, sediment depth,
71 along with trapping systems such as macrophytes (House & Warwick, 1999) or man-made
72 structures. In addition, the locations and type of P inputs (e.g. STWs and soil erosion) will
73 determine inputs of P into the river or estuary. For example, recent work by Tye et al. (2016)
74 on the non-tidal river Nene demonstrated an increase in sediment P concentrations with

distance from the head waters, with point sources (STW's) and the increasing urbanisation of the catchment being considered a major influence on the increasing P sediment concentration.

One area of P storage within estuaries which have received less attention than salt marsh sediments are foreshore or inter-tidal mudflats. Whereas, salt marsh sediments are considered relatively efficient sinks for nutrients (Coelho et al. 2004), fore-shore mudflats differ in that they are devoid of vegetation and undergo submersion twice a day. They represent a temporary storage zone, but like salt marsh sediments have the potential to supply the water column with P either through mineralisation or P desorption (Coelho et al. 2004; Mortimer et al. 1998; Wang and Li, 2010). Mudflats undergo cycles of deposition and erosion over differing timescales with their elevation and morphology controlled by tidal forcing and river discharge (Baugh et al. 2013). In addition, wind events and biological activity may complicate the deposition and erosion events (Deloffre et al. 2007). Phosphorus interactions with sediment in tidal sections of rivers are known to differ markedly from those in fresh water (House et al. 1998; Sundareshwar and Morris, 1999). This is largely through the role of increasing salinity and ionic strength that leads to the release of sediment bound P and flocculation of suspended sediments in the turbidity maximum (House et al. 1998). Phosphorus stored within these sediments can exist in many forms including inorganic P species, organic P species and in mineral phases such as calcium phosphate (apatite) or vivianite. Redox changes can either initiate the release or fixation of P from oxide phases (Reddy et al. 1995; House & Dension, 2000). Sulphate may also influence the release of P from Fe oxide phases leading to the recycling of sediment P (Caraco et al. 1989). The release of sediment P may be through the Equilibrium Phosphorus Concentration (EPC_0) model (Froelich, 1988). These processes may contribute to increasing P concentrations in estuarine waters and export to the oceans (Fox et al. 1986; Lebo and Sharp, 1992) where biological

100 uptake and recycling are intensive, especially if N is not limited (Correll, 1998). This can lead
101 to changes in the speciation of suspended sediment and particulate P which can be seasonally
102 influenced (Zwolsman, 1994).
103
104 This paper investigates the controls on P concentration and speciation within the inter-tidal
105 mudflats of the tidal River Thames, UK, a major UK river which flows through London.
106 Recent work by Powers et al (2016) produced a history of P fluxes (Kt yr^{-1}) within the
107 Thames catchment and demonstrated that between 1940 and 1980, inputs of P into the
108 catchment in order of importance, were fertiliser P, food/feed export from farms, food waste
109 to landfill and P input from sewage to treatment works. These were found to greatly exceed
110 river export. However, since the late 1990's, and during the 2000's, gross annual exports
111 from the landscape pool (land & river) of the Thames basin have slightly exceeded inputs.
112 However, the results described by Powers et al. (2016) demonstrate how in the
113 Anthropocene, the P cycle within catchments is dominated by human inputs which greatly
114 exceed fluvial export and that substantial P is stored within components of the catchment.
115 Whereas much work has been undertaken on the controls on P and improvements resulting
116 from P stripping in STW's of the upper Thames catchment (Neal et al. 2000; Neal et al. 2010;
117 Neal et al. 2006), this work examines the tidal section that flows through central London to
118 the North Sea, and where significant P is released from some of the largest STW's in Europe.
119 As the tidal mudflat sediments are formed through the sedimentation of suspended sediment,
120 they present an archive of the environmental effects on suspended sediment P interactions

and secondly on those processes when sediment P is in temporary storage within the mudflat. By combining data on the concentration and speciation of P with knowledge of the sediment transport system, a broad conceptual understanding of P cycling can be made for the tidal Thames.

2. Materials and Methods

2.1 Study area

The river Thames is the UK's longest river with a length of 345 km, a catchment area of 12935 km^2 and with an average discharge of 65.8 $m^3 s^{-1}$ (Marsh and Hannaford, 2008). The rural upper catchment consists largely of agricultural land on limestone and chalk geology, flowing through a succession of large towns / small cities, before flowing through the centre of the city of London and out to the North Sea (Figure 1). The fore-shore mud flat sediments examined in this work are from the tidal section of the Thames which consists of a 120 km section from Teddington Lock in west London to the Essex coastline.

To understand the dynamics of P storage within these fore-shore sediments, understanding of (i) the origin of the sediments, (ii) their movement and (iii) inputs of P into the system is required. There are two main sources of sediment within the tidal river, these (i) originating from the catchment upstream of Teddington, and (ii) the tidal remobilisation of sediment in the estuary and transport upstream. Littlewood and Crossman (2003) provide an indication as to the extent that particles may travel. They suggest that if a particle started at Southend (Core 46; Fig 1) it may move upstream 12 km on a large spring tide and 17 km if the particle started at Greenwich (Core 14; Fig 1). However, suspended sediment would only drop out to form the mud-flats when current velocity and particle size are appropriate. Deposited sediment may erode when the critical threshold for re-mobilization is next achieved. The movement of sediment in suspension will be greatest on spring tides and least on neap tides,

due to the greater forces produced by the spring tide. In addition to the suspended load, a great deal of sediment is transported upstream as near bed load where high concentrations and fluxes can occur. It would appear that this process is driven by salinity gradients and freshwater flow. Thus, in periods of low fresh water flow (April to September) the average

150 salinity in the Blackwall Point and Lower Gravesend reach increases as it does not undergo
151 as much dilution from the fluvial flow. This seasonal salinity change results in sediment
152 being moved upstream and deposition occurring, where the salinity and flow velocity are
153 suitable. This is a slow process and takes several months. In autumn, the increased fresh
154 water flow may re-mobilise cohesive bed sediments. Results suggest that most of this
155 sediment moves at very high concentration in the deepest parts of the channel, with only a
156 small part of the sediment rising into suspension. However, within a few days this downward
157 channel movement of sediment can reverse the whole of the summer period upstream
158 transport.
159 We have divided the tidal Thames into four zones based on suspended sediment
160 concentrations by Littlewood and Crossman (2003). Zone 1 stretches from Teddington Lock
161 to Lower Pool (Cores 1-12) and in this stretch the suspended sediment concentrations are
162 generally low with concentrations at Putney (17 km from Teddington of 40-120 mg L^{-1} and at
163 Vauxhall Bridge (27 km from Teddington Lock) of 60-140 mg L^{-1}. Within this zone there is
164 little deposition of sediment on the banks of the river with much of the sediment passing
165 through. Zone 2 (Cores 13-27) covers the distance between Lower Pool to Erith Reach (24
166 km) and includes the turbidity maximum around Gallions, Barking and Halfway reaches
167 (Cores 17-27). Traditionally these are known as the ‘mud reaches’ as this is the limit of saline
168 intrusion which causes flocculation and deposition of the sediment. The position of the
169 turbidity maximum is liable to fluctuate with tidal range, sea level changes and the seasonal
170 change in freshwater and saline tidal flow. The movement of this saline front has a

fundamental effect on the deposition of sediment. During winter, when river flow is high, the saline water front is pushed back and this causes the sediment to be flushed out of the 'Mud Reaches' and stored in the Gravesend Reach area of Zone 3 (Cores 30-32). In the summer when river flow is lower the saline front moves back upstream, which again starts the process

of flocculation and deposition of the sediments. The suspended sediment concentrations are highest in this zone with concentrations at Barking in the range 500-600 mg kg^{-1}. Zone 3 (Cores 28-33) occupies the distance from Erith to Lower Gravesend Reach (20 km) and generally has moderately high suspended sediment concentrations with concentrations at Tilbury between 200-400 mg L^{-1}. Zone 4 (Cores 34-47) is the area between Gravesend to Sea Reach spans a distance of 27 km and connects the estuary to southern North Sea. Combined with these general sediment dynamics are inputs of dissolved and particulate P. In Zone 1, P inputs will be from the agriculture and STW's sited in the upstream catchment. Within Zone 1 there are additional major inputs from the STW at Mogden. In Zone 2, there are three major STW's including those at Becton, Crossness and Riverside, whilst in Zone 3 there is the Long Reach STW. In addition, to P discharges from all these STW's sewage is discharged into the Thames via overflow sewers during times of heavy rainfall.

2.2 Sediment Sampling

Two sets of sediment were collected, (i) sediment cores (n=47) collected in non-sequential order in November 2009, October 2010 and November 2011 from zones 1-4 and (ii) a further 23 surface grab samples (2-5cm deep), representing the most recently deposited sediments and were collected using a stainless steel trowel from zones 1 and 2 in November 2011. Sample positions of cores (C) and surface grab samples (G) are shown in Figures 1 and 2 respectively.

Inter-tidal sampling sites were accessed by Port of London Authority Dory attached to the

197 vessel Driftwood II, using pre-determined GPS co-ordinates (Vane *et al*., 2015). At each core

198 site, clear polycarbonate tubes (140 cm length × 6 cm I.D) fitted with a stainless steel basket

199 catcher at the base were manually driven into the exposed sediment and extracted to recover

200 the core material (Vane *et al*., 2011; Vane *et al*. 2007). Sediments were frozen at -18° C
201 within 3 h of exhumation and transported frozen in the dark from London to the BGS
202 laboratories to avoid post-collection chemical changes and physical movement. Upon receipt
203 each core was cut longitudinally in half and sliced into 10 cm intervals (Vane *et al*., 2013).
204 The resultant sediment samples were freeze-dried, disaggregated, sieved to pass a 2 mm
205 mesh. A subsample of the < 2mm fraction was ground to a fine powder using an agate ball-
206 mill (Beriro *et al*. 2014). Prepared Thames sediments were subsequently stored in the dark at
207 14°C in sealed polyethylene bags. All samples were thoroughly mixed to avoid
208 inhomogeneity caused by density settling during storage.
209

210 **2.3 Analytical Methods**

211 Total element concentrations in the sediment cores were determined using XRFS
212 Spectrometer using the same analytical method, instrumentation and calibration package as
213 previously reported for mangrove sediments (Vane *et al*., 2009). TOC was determined using
214 a Europa Scientific Elemental Analyser, after samples were treated with 1M HCl, and washed
215 with deionised water to remove inorganic C, before being oven dried at 60°C (Lopes dos
216 Santos and Vane, 2016). Estimates of poorly crystalline oxyhydroxides of Fe (FeOOH), Mn
217 (MnO_x) and Al (AlOOH) in sediment were determined using 0.2M ammonium oxalate and
218 0.125M oxalic acid extractions. Samples were shaken in darkness for 2 hours (McKeague &
219 Day, 1966), centrifuged at 3500 rpm and filtered (0.45µm nylon syringe filters) before
220 analysis by ICP-AES. Using results from the oxalate extraction the Degree Phosphrous

221 Saturation (% DPS) can be estimated as $P_{Oxalate}/(Fe_{Oxalate} + Al_{Oxalate})*100$. Estimates of Total

222 Organic Phosphorus were made by extracting samples using 0.25M NaOH and 0.05M EDTA

223 for 16 hours at 20°C (Turner et al. 2003). After extraction sub-samples were analysed for (i)

224 'Inorganic P (molybdate reactive P)' ($P_{Inorganic}$) and (ii) total P with estimates of organic P

225 ($P_{Organic}$) being the difference between the two measurements. $P_{Inorganic}$ was measured by
226 molybdate blue immediately after extraction and Total P in the extracts was measured by
227 ICP-AES. Methodological constraints have been discussed in previous work (Worsfield et al.,
228 2008). It is possible that the within $P_{Inorganic}$ measurement some acid hydrolysable organic and
229 condensed P may be included through the molybdate blue analysis and within $P_{Organic}$
230 measurement some inorganic polyphosphates may be measured (Turner et al. 2003). Samples
231 were analysed in batches of 30, with two samples selected that were extracted and analysed in
232 every batch. These were samples core 41 (20-30 cm) and core 35 (10-20 cm). For the $P_{Inorganic}$
233 measurement the nine replicates from core 41 gave a mean concentration of 448 mg kg^{-1} ±
234 SD = 16.36 (% CV = 3.64; n=9) and for core sample 35 a mean concentration of 805 mg kg^{-1} ± SD = 38.88 (% CV 4.83, n=9). For the ICP-AES measurement of Total P in NaOH
236 solutions, the core 41 sample gave a mean concentration of 495.6 mg kg^{-1} ± SD 23.1 (% CV
237 = 4.66 %; n=9) and core sample 35 gave a mean concentration of 878.2 mg kg^{-1} ± SD 17.28
238 (% CV = 1.97; n=9). In some samples $P_{Inorganic}$ was found to be equal or slightly greater than
239 the ICP-AES measurement thereby returning a negative $P_{Organic}$ value. This is probably
240 associated with experimental (e.g. Worsfield et al, 2008) and analytical error associated with
241 each method. Therefore an 'uncertainty propagation' analysis was undertaken for samples,
242 using information obtained from the replicates samples and based on 95 % Confidence
243 Intervals to ascertain samples which had a robust and identifiable $P_{Organic}$ concentration.
244 Results suggested that those $P_{Organic}$ concentrations < 21 mg kg^{-1} were not sufficiently robust
245 and were therefore not included within the dataset.
246

247 Scanning electron microscopy (SEM) was undertaken to characterise the sediments and
248 identify P containing mineral phases. Sub samples of sediment were mounted on stubs and
249 were coated with a thin film of carbon approximately 25 nm thick using an EMITECH 960L

250 evaporation-coating unit. Analyses were performed using a LEO 435VP variable pressure
251 SEM, and an FEI Quanta 600 environmental SEM, under high vacuum (<1x10-4 Torr) and
252 variable vacuum (0.45 Torr water atmosphere) conditions respectively. Accelerating voltages
253 of 20kV were used in both. SEM photomicrographs were obtained under backscatter electron
254 imaging (BSEM) and secondary electron imaging (SE) conditions as 8 bit greyscale TIF
255 format digital images. Phase/mineral identification was aided by qualitative observation of
256 energy-dispersive X-ray spectra recorded simultaneously during SEM analysis, using Oxford
257 Instruments INCA energy-dispersive X-ray microanalysis (EDXA) systems. One core from
258 each of the 4 sediment zones of the tidal Thames were selected and three depths analysed,
259 these being:

260 Zone 1 – Core TH29, 10-20 cm, 30-40 cm and 60-70cm

261 Zone 2 – Core THS3, 0-10 cm, 30-40 cm and 50 -60 cm

262 Zone 3 – Core TH10, 10-20 cm, 40-50 cm and 70-80 cm

263 Zone 4 – Core TH2, depths 10-20 cm, 30-40 cm 50 – 60 cm

264

265 **3. Results and Discussion**

266 **3.1 Sediment characteristics**

267 It is important to assess the geochemical characteristics of the sediment prior to examining
268 changes in the P concentrations and speciation. This is to ensure that a change of sediment
269 source is not responsible for the changes in P properties. For example, it has been suggested
270 that the Thames estuary may receive sediment from sources such as the North Norfolk coast

where extensive cliff erosion occurs. Total mean concentrations of Al and Si for each core were determined from the 10 cm sections, and used as proxies of alumina-silicate minerals, so that geochemical relationships of the sediment between the inner and outer estuary zones could be examined. Results showed that there was reasonable consistency in Si and Al

concentrations, along the length of the Thames estuary (Figures 3a & 3b). There was possibly greater variation in Zone 1 cores closer to Teddington Lock, possibly because of less tidal mixing further up the river. A further test to assess changes in sediment source was to examine the relationship between Al and Rb, with the hypothesis that clay minerals derived from different sources would have different Al:Rb ratios (assuming that a significant proportion of the Al present was as clay minerals and that Rb is largely present in the clay minerals). Figure 3 shows a very strong correlation (r^2 = 0.95) between Al and Rb for the whole dataset, suggesting that the sediment is likely from a similar source or is well mixed within the estuary before sedimentation. Similarly strong correlations were found between other clay components including K v Ti (R^2=0.92), Ti v Al (R^2 =0.97) and Ti v Mg (R^2 =0.89). There appeared to be no definite trend in sediment depth throughout the estuary although depths varied from 10 cm to >1m (Figure 4a).

3.2 Total Phosphorus in foreshore sediments

Results from the sediment geochemical analysis suggest that (i) the sediment collected from the fore-shore appeared to be from one source (or thoroughly mixed) and that there was not a distinctive fining of the sediment towards the estuary mouth. Both of these factors could influence P_{Total} distribution, but based on these results it does not appear that they have a large influence. Using the sediment zone classification of Littlewood and Crossman (2003) and described in the Material and Methods, mean P_{Total} concentration in each core was determined by averaging the 10 cm depth increments. These were then plotted against their

296 distance from Teddington Lock (Figure 4c). It is evident that mean P_{Total} concentrations were

297 highest in Zones 1 and 2 with a large fall in concentrations in Zone 3 and 4. When compared

298 to the salinity concentrations transect (Figure 4b) taken from the data of Pope and Langston

(2011), it can be seen that the decrease in P_{Total} concentrations in Zones 3 & 4, occurs when there is an increase in salinity above ~6 ppt.

Figure 5 shows the variation of P_{Total} concentrations within the 0-10 cm sections from cores from each of the 4 sediment zones using Box and Whisker plots, along with the grab samples taken from Zones 1 and 2. The greatest variation and range of P_{Total} concentrations were found in Zone 1, possibly because there is less mixing of sediment towards the tidal limit (Teddington Lock). For Zone 2, the range of P_{Total} concentrations was smaller than in Zone 1 and the P_{Total} concentrations between the 25^{th} – 75^{th} percentiles showed less variation than in Zone 1. For Zones 3 and 4, it was evident that the concentration ranges of P were greatly reduced compared to Zones 1 and 2, and with less variation, particularly between the 25^{th} and 75^{th} percentiles. Median values for the grab samples from Zone 1 and 2 were higher than the mean P_{Total} concentrations in the cores taken from their respective zones, but the distribution of concentrations were broadly similar. Thus the grab samples did not demonstrate that the P_{Total} concentrations in the most recently deposited sediments were significantly different from the core sample concentrations. The reasonably consistent concentrations of P_{Total} within the 25^{th} to 75^{th} percentiles ranges in the cores from each zone probably reflects the (i) thorough sediment mixing due to the strong? tidal cycle (see Section 2.1), storm events and anthropogenic physical disturbance (e.g. maintenance dredging) and (ii) the controls that water properties (e.g. salinity) may produce.

The relationships between P_{Total} and the elements it is likely to form mineral phases with or act as a binding surface with were examined. Initial exploration of the data (n=279 samples)

identified a series of outliers which prevented models involving P_{Total} to parameterise effectively. These outliers were removed from the dataset, prior to further P_{Total} data analysis. Core 29 (Rainham) values were removed as this core came from was a salt marsh sample,

rather than a foreshore mudflat sediment, and because its environmental setting led it to have very different geochemical properties. There were also a series of samples (n=20) where Fe_{Total} concentrations were > 60 000 mg kg^{-1}. The values removed came largely from core 32 (Shorne, n=5), core 24 (Crossness, n=4), core 33 (Cliffe, n=2), core 25 (Dagenham Ford Pier, n=3), and core 28 (Dartford, n=3) with individual values coming from 2 (Chiswick Bridge), 13 (Deptford Creek) and 10 (Vauxhall Bridge). These samples also had elevated concentrations of trace metals, compared to the remaining dataset. For Cores 24, 25, 32 and 33 these included V and Co suggesting that the higher concentrations of Fe in these samples may have been derived from metallurgical industries.

After removing these 20 samples, reasonably strong relationships between P and TOC (r=0.77) and Mn (r=0.76) with P_{Total} were found (Figure 6). Generally, poor relationships were found between Fe_{Total}, Al_{Total} and Ca_{Total} and P_{Total}. To further understand the geochemical associations of P, SEM analysis of selected cores samples (Section 2.3) were undertaken. All samples analysed contained mainly silicates, with some Ca carbonates (mostly as coccoliths) and iron-titanium phases (ilmenite) being present. However, the mineral phase which was ubiquitous was pyrite (FeS_2) suggesting the presence of reducing conditions throughout the cores examined from the four different zones (Figure 7). Minerals containing P were rare in all the samples examined. However, occasional P containing minerals were found. For example, in core 2 (Zone 1) at a depth of 30-40 cm, a small fragment of apatite included within a mica (biotite) sheet was found. In core 26 (Zone 2), at a

depth of 0-10 cm there was an altered Fe mineral, with a small concentration of P present, along with some infrequent apatite. At a depth 50-60 cm a rare-earth phosphate-mineral was found (aluminium-strontium–phosphate + rare earths). At a depth of 40-50 cm, a particle of amorphous Fe oxide containing very small concentrations of Mn and P was found. Possible

vivianite (dominant detectable elements are Fe, P and O, with lesser Mn) was recognised in core 36 (Zone 4), at depths of 10-20 cm and 30-40 cm.

A regression model to determine the key variables that may explain the concentration of P_{Total} in the dataset (n=224) was parameterised. The best fit model for predicting P_{Total} had an adjusted R^2 of 0.80 and is presented in Table 1, with the observed v predicted values shown in Figure 8. The three significant (P<0.001) co-variables of the model were Mn_{Total}, TOC and salinity. It is likely that Mn_{Total} was significant as it is likely linked to the Fe(III) oxy-hydroxides that are involved in P adsorption and the positive relationship with TOC was likely because much of the P is released from STW's or sewerage overflow which also are likely to release organic matter. Salinity is included because of the role increasing anion (e.g. sulphate) concentrations may have on desorption of P species from the sediment (Caraco et al. 1989).

3.3 Oxalate Extractable P and non-crystalline oxides

All core samples and grab samples were analysed for $P_{Oxalate}$, an estimate of the P associated with the non-crystalline oxides of $Al_{Oxalate}$, $Fe_{Oxalate}$ and $Mn_{Oxalate}$, either being surface bound or fixed within the poorly crystalline oxide structure. Measurements are also likely to include P associated with the release of organic species, originally bound to the non-crystalline oxide phases (Basile-Doelsch et al., 2015). The relationships between Total Fe, Al and Mn and their oxalate extractable oxide phases (Figure 9) show that for $Fe_{Oxalate}$ and $Al_{Oxalate}$ the effects of salinity are apparent; there being a higher proportion of $Fe_{Oxalate}$ and $Al_{Oxalate}$ in sediment

370 Zones 1 and 2, than in Zones 3 and 4 where salinity is increasing, whilst the range of Fe_{Total}

371 and Al_{Total} are broadly similar. For $Fe_{Oxalate}$ this may suggest that the increasing sulphate

372 concentrations associated with salinity is producing FeS_2 (Caraco et al., 1989). For $Mn_{Oxalate}$,

373 a linear relationship ($R^2 = 0.87$) was found with Mn_{Total} for the entire dataset.

Data showed that $P_{Oxalate}$ concentrations were broadly similar in pattern to P_{Total} with distance from Teddington Lock. Figure 10 shows the relationship between P_{Total} v $P_{Oxalate}$ and demonstrates that for many samples the oxalate extraction removes a significant proportion of P_{Total}, with an overall relationship being:

$$P_{Oxalate} = 0.9765*P_{Total} - 347.2; \qquad R^2 = 0.88 \qquad \text{eqn. 1}$$

It was found that $P_{Oxalate}$ slightly exceeded P_{Total} in a small number of samples with the highest P_{Total} concentrations, these being from Zone 2 where the major STW's are sited. This is likely to occur when $P_{Oxalate}$ accounts for most of the P present along with any analytical error associated with ICP-AES measurements. The $P_{Oxalate}$:P_{Total} ratios found in the different sediment zones of the Thames was explored. A higher proportion of P was oxalate extractable in Zones 1 and 2 than in Zones 3 and 4 (Figure 11). Median $P_{Oxalate}$:P_{Total} in zones 1 and 2 was ~0.8 whilst in Zones 3 and 4 median values ~0.6. In addition, it was also obvious that those samples in Zones 3 and 4 generally had a more constrained distribution around the median value than samples in Zones 1 and 2. The suggestion from these results is that samples from Zones 1 and 2 have a lot of surface adsorbed P, possibly as a result of discharges from the STW's present but in Zones 3 and 4, this has been desorbed because of the increase in salinity. Correlations between $P_{Oxalate}$ and the non-crystalline oxides were assessed for the whole dataset (Figure 12). There were strong correlations between $Fe_{Oxalate}$ (r=0.89) and $Mn_{Oxalate}$ (r=0.79) and $P_{Oxalate}$, with a lesser correlation with $Al_{Oxalate}$. In

ad dition, $Mn_{Oxalate}$ and $Fe_{Oxalate}$ showed a strong correlation (r=0.80).

396 The degree of phosphorous saturation (DPS) was examined to assess whether the decrease in

397 the proportion of non-crystalline oxide surfaces found in Zones 3 and 4 are likely to be a

398 constraint on phosphate sorption. In Figure 13, box and whisker plots show the % DSP for

399 core samples in each zone and also from the grab samples taken from Zones 1 and 2. There
400 was generally a lower % DPS in Zones 3 and 4 than in Zones 1 and 2. Median values of %
401 DPS in Zones 1 and 2 were between 20 -30 %, whilst for Zones 3 and 4 they were between
402 10-15 %, suggesting that there is potential for further sorption in all zones.
403
404 A model to predict the concentration of $P_{Oxalate}$ was parameterised and results can be seen in
405 Table 2 and Figure 14. In parameterising the model, the possible effects of salinity were
406 considered as it is likely responsible for both desorption of phosphate species and also the
407 lower proportion of non-crystalline oxides of Fe an Al that phosphates may bind too.
408 Analysis of data showed weak negative correlations between salinity and $Fe_{Oxalate}$ (r=-0.35)
409 and $Al_{Oxalate}$ (r=-0.51), suggesting that some interactions were present. Therefore, whilst a
410 predictive model can be parametrised this small cross-correlation means that a comparison of
411 the coefficients and their relative importance cannot be undertaken. Two models were
412 parameterised, firstly one using the three oxalate oxide phases (Fe, Mn, Al) which had an
413 adjusted R^2 of 0.75 and a second, where salinity was included with an R^2 of 0.80.
414 Undertaking an ANOVA to compare the two model outputs it was found that the second
415 model with salinity included was significantly (P<0.001) improved and is the one presented
416 in Table 2 and Figure 14.
417

418 **3.4 Estimates of NaOH extractable inorganic and organic P**

419 Whereas the estimates of $P_{Oxalate}$ include inorganic and organic P associated with amorphous

or non-crystalline oxides, improved estimates of inorganic and organic species were examined using the P_{NaOH} extraction. Concentrations of $NaOH_{Total}$ were related to P_{Total} and $P_{Oxalate}$ through the following equations:

$$\text{Total NaOH P} = 0.7208 * P_{Total};\ R^2=0.91 \qquad \text{eqn. 2}$$

Total NaOH P = 0.8060 *$P_{Oxalate}$; R^2 =0.94 eqn. 3

The equations demonstrate that the combined $P_{Inorganic}$ and $P_{Organic}$ fractions extracted using NaOH represent significant proportions of both the P_{Total} and $P_{Oxalate}$ pools. A general pattern existed for the NaOH extractable Inorganic and Organic P pools in that when $P_{Inorganic}$ was typically < 1000 mg kg^{-1}, the concentrations of $P_{Organic}$ were generally also low or below analytical detection. Thereafter as $P_{Inorganic}$ increases there was a concomitant increase in $P_{Organic}$ concentrations which often exceed the $P_{Inorganic}$, concentration. Figure 15 shows how concentrations of both $P_{Inorganic}$ and $P_{Organic}$ vary with distance from Teddington Lock, at three depth intervals; these being 0-10 cm, 30-40 cm and 50-60 cm. Missing values indicate that sediment was not present at that depth. Two trends can be seen in the data. Firstly, in zones 1 and 2, concentrations of $P_{Organic}$ were generally a higher proportion of the P extracted with NaOH than in zones 3 and 4 at all three depths, with the exception of TH7 which was the core taken on the salt marsh. The second trend shows that a substantial concentration of $P_{Organic}$ in zones 1 and 2 remains with increasing depth. In a similar manner to the $P_{Oxalate}$ model, two models were parameterised, one without salinity and one where salinity was included, because of the possible effects of salinity on the oxide surfaces and desorption of P. Model one predicted $P_{Inorganic}$ using $Mn_{Oxalate}$ and $Fe_{Oxalate}$ and had a R^2 of 0.69. The inclusion of salinity to the above model increased the adjusted R^2 to 0.76 and is reported in Table 3 and Figure 16. An ANOVA comparing the two models showed that the second model was significantly (P<0.001) improved by including salinity.

Discussion

446 The inter-tidal mud flats of the River Thames represent a temporary storage component for
447 sediment associated P within the estuarine system, but one which is vulnerable to
448 remobilisation, with the potential for the release of P to estuarine waters. Thus evidence from

449 the spatial distribution and speciation of P in the intertidal mud flat sediments of the River
450 Thames combined with existing information regarding salinity and sediment movement can
451 be combined to provide a conceptual understanding of sediment-P release to water and
452 storage (Figure 17). The fore-shore sediments are formed from deposited suspended sediment
453 and therefore concentrations and speciation of deposited sediment-P are likely to reflect (i)
454 the interactions between suspended sediment and the estuarine / river aquatic environment at
455 the point of deposition and (ii) in-situ processes once it has settled. Results for the Thames
456 suggest that the P concentrations and speciation in the intertidal muds can be considered in
457 the context of the four suspended sediment zones suggested by Littlewood and Crossman
458 (2003). These sections all differ in P inputs and environmental gradients (salinity, SPM).
459 Zones 1 & 2 have large inputs of P from 4 major London STW's (Mogden, Abbey Mills
460 CSO, Beckton and Crossness) combined with P originating from the catchment above
461 Teddington lock, whereas Zones 3 & 4 represent an increasingly saline environment. Zone 2
462 generally had the most samples with high concentrations of P in the 25-75th percentile range,
463 probably as a result of the STW inputs. Previous work on these core samples have suggested
464 that the highest concentrations of the biomarker crenarchaeol, an indicator of ammonia-
465 oxidising Thaumarchaeota were found in this zone (Lopes dos Santos & Vane, 2016). This
466 Archaea has been found in STW effluent (Kim et al. 2007). Thereafter the two dominant
467 factors to be considered when accounting for the change in sediment P distribution and
468 speciation through the tidal river system are (i) sediment source and transport and (ii) salinity.
469

With respect to sediment source, several authors (e.g. Inglis & Allen, 1957; WPRL, 1964) who undertook sediment budgets have suggested that inputs from the wider coastline, particularly from the decay of cliffs north of the Thames estuary, were needed to balance sediment budgets for the Thames estuary. However, recent work by Baugh et al. (2013), who

474 undertook a fine sediment budget for the Thames, suggests that no large marine source of
475 sediment is required to balance the sediment budget. This concurs with the initial assessment
476 of sediment geochemical relationships undertaken in this work. Correlations (r=>0.95) were
477 found for the whole dataset for the major elements K, Rb, Mg, Al, and Ti, which typically
478 make up the clay fraction. In addition the statistical relationships for these elements were not
479 found to be different when zones 1 and 2 and zones 3 and 4 were compared, indicating that
480 the geochemistry of the sediment samples largely represent a single source of well mixed
481 sediment present throughout the estuary. One aspect of estuarine sediment movement that
482 may enhance sediment mixing is the sediment shuttle that operates between zones 2, 3 and 4
483 and which was identified by Ingliss & Allen (1957) who used ^{46}Sc to track the movement of
484 sediment in the Thames. This mixing of sediment is likely one reason for the relatively
485 consistent P_{Total} concentrations found in each sediment zone, particularly between the 25^{th}
486 and 75^{th} percentiles. Having ascertained that a change in sediment source is not the likely
487 cause for changes in sediment P concentrations, other processes can be examined. Two key
488 mechanisms can be considered, these being the interactions between (i) salinity and
489 suspended sediment P before deposition and (ii) P interactions with salinity within the
490 deposited sediment.
491
492 Previous work (e.g. Upchurch et al. 1974; Fox et al. 1986; Jordan et al. 2008; Zhang and
493 Huang, 2011) suggests that salinity is a key control in the distribution and speciation of P
494 within a river-estuary system, especially within the turbidity maximum and as suspended
495 sediment passes from fresh to saline water. Desorption of surface adsorbed sediment P has

been found as salinity increases (Upchurch et al. 1974; Deborde et al. 2007; Lebo, 1991), largely through increased ionic strength and competition from other anions (e.g. OH^-, F^-, SO_4^- and $B(OH)_4^-$) for sorption sites (Froelich, 1988). For example, Deborde et al. (2007)

found a decrease in both organic and easily exchangeable inorganic P in suspended sediment along a salinity gradient in the Gironde estuary in France. Salinity also influences sediment P concentration and speciation within the mud flat deposits because of the role sulphide plays in releasing phosphate. This is via the dissolution of Fe-P complexes and the formation of FeS_2 minerals (Krom and Berner, 1980; Caraco et al. 1989; Jensen et al. 1995). In addition, once deposited as mudflat sediment P sorption or desorption will be dependent on the Equilibrium Phosphate Concentration (EPC_0). The EPC_0 determines the potential of P desorption or adsorption of deposited sediment in relation to the concentration of P in the river water. Zhang and Huang, (2011) demonstrated that only minor differences were found in EPC values with salinities varying between 2-9 ppt. However EPC increased thereafter as salinity increased.

Within the Thames estuary salinity had the greatest influence on the interactions between sediment-P and its environment especially as the % DPS demonstrated sufficient oxide surfaces for P sorption, even in zones 3 and 4 where there was a lower proportion of oxide surfaces. Evidence of the salinity gradient on P desorption was found to be significant within the models predicting P_{Total}, and $P_{Oxalate}$, and $P_{Inorganic}$. In particular, as salinity increases to 6 ppt at the beginning of Zone 3 major changes in the concentration and speciation of P in the Thames sediments occurs. A secondary influence on P desorption may also be produced by the concentration of Suspended Particulate Matter (SPM), which also changes with salinity. Deborde et al. (2007) demonstrated in laboratory experiments that the salinity at which P

desorption occurs changed with suspended sediment concentrations. When suspended sediment concentrations were low (< 83 mg L^{-1} SS) desorption occurred in the salinity range 0-3 ppt whilst with higher suspended sediment concentrations (when = or > 500 mg L^{-1})

523 desorption occurred 0-15 ppt. Thus the suggestion is that at higher SPM concentrations,
524 desorption of P may occur at a higher salinity.
525 Examining the interactions between salinity and SPM with respect to the Thames mudflat
526 sediments, conditions for P desorption from the sediment can be estimated (Figure 17). For
527 the Thames, Uncles and Mitchell (2011) suggest an average surface salinity in the Estuarine
528 Turbidity Maximum (ETM) of ~3 ppt, with its average position being between the Millenium
529 Dome and Woolwich Reach (between Cores 15 and 14; Zone 2). Various reports have been
530 published for suspended sediment concentrations in the ETM of the Thames (e.g. Uncles and
531 Mitchell, 2011). However, Baugh & Littlewood (2005) suggested tidally and width averaged
532 ETM SPM concentrations of approx. 600 and 150 mg L^{-1} at spring and Neap tides
533 respectively. After the turbidity maximum, salinity rises to 4 ppt in Zone 2. However, P
534 desorption does not appear to occur in Zone 2, Thus the SPM concentrations in Zone 2 may
535 be sufficient to reduce P desorption as suggested by Deborde et al. (2007), even though the
536 salinity has increased beyond the 3 ppt suggested for water with low SPM concentrations. In
537 the Thames, P desorption from sediment appears to occur at the interface between Zones 2
538 and 3 (Cores 27 and 28). Reported environmental conditions where this occurs based on data
539 from Uncles and Mitchell (2011) and Pope and Langston (2011) are a surface water SPM
540 decline to less than 50 mg L^{-1} and a salinity increase from 4 - 6 ppt. These figures are a
541 reasonable approximation of those given by Deborde et al. (2007), but demonstrate how the
542 interaction between SPM concentrations and salinity may determine conditions for P
543 desorption. Importantly, Deborde (2007) also suggested that P desorption was irrespective of

544 pre-existing P concentrations in saline waters. It is likely that desorption of P from the

545 Thames SPM occurs in waters with mean annual P concentrations that far exceed the Water

546 Framework Directive standard (< 120 ug L^{-1}) required for Good Ecological Status in fresh

547 waters (lowland, high alkalinity) (Defra, 2014). In summer and autumn, seasonal mean

548 concentrations of 1500 and 1800 µg L^{-1} have been reported in the Thames Tideway (Thames
549 Water Utilities Ltd, 2011). In addition, the Cross Ness STW, one of the largest in Europe
550 discharges into the Thames only 5 km upstream of Zone 3. Data extracted from the EA
551 WIMS (http://environment.data.gov.uk/water-quality/view/download) database for 2015
552 provide measurements of orthophosphate concentrations from Hammersmith Bridge (Core 4)
553 to the ocean. Data suggests the mean value for 2015 (n=6) is ~1 mg L^{-1} for Zones 1 and 2,
554 with a drop in orthophosphate to 0.5 mg L^{-1} by the end of Zone 3 and a concentration of <0.1
555 mg L^{-1} in Zone 4. Thus the suggestion is that P desorption occurs in waters with P
556 concentrations of between 0.5 – 1 mg L^{-1}.
557

558 The salinity gradient also appeared to influence P speciation. This was demonstrated by both
559 the $P_{Oxalate}$ and P_{NaOH} results. Results demonstrated that although approximately 70 % of the
560 P_{Total} was held as P_{NaOH} extractable species throughout the tidal Thames (Equation 2), the
561 proportion of inorganic and organic species appeared to change with increasing distance from
562 Teddington Lock. In Zones 1 and 2, a greater proportion of organic P was generally found
563 compared to samples from Zones 3 and 4, where P appeared to be predominantly inorganic
564 MRP. Organic P is likely to be surface adsorbed, but binds less strongly than inorganic MRP,
565 leading to its likely preferential desorption in saline waters (Gardolinski et al., 2004;
566 Ruttenberg & Sulak, 2011). The source of much of this $P_{Organic}$ is likely to be outputs from
567 the STW's in Zones 1 and 2. However, evidence from the different depths reported (Figure
568 13) suggest that organic P remained a significant proportion of NaOH extractable P, even at
569 depths as deep as 70 cm in zones 1 and 2.

The presence of P_{O} at

Comment [LD1]:

570 suggests that it has not been utilised by bacteria. In freshwater lakes Reitzel et al. (2007)

571 found organic P species including orthophosphate monoesters and orthophosphate diesters

572 including Teichoic acid and DNA-P to sediment depths of 40 cm, and dated to ~100 yrs old.

573 However, without further speciation of the organic P fraction using techniques such as ^{31}P

574 NMR, it is not possible to speculate further on these sources and processes.

575 Examination of the mineral phases using SEM analysis demonstrated the relative paucity of P

576 containing mineral phases in each of the 4 zones, but particularly in zones 3 and 4. There was

577 a general absence of identifiable Fe-Mn-P oxide minerals that have been identified in

578 freshwater river systems (Tye et al. 2016), possibly suggesting that the absence of plant roots

579 prevents the distribution of oxygen required within the sediment to create large mineral

580 surfaces for P sorption (Christensen et al. 1997). In addition, no definite identification of

581 Vivianite minerals were found, which are typical of reduced sediments in freshwater and act

582 as a sink for P within the sediment. However, the ubiquitous presence of FeS_2 phases,

583 suggest that Fe is precipitating as FeS_2 minerals in preference to Vivianite in this saline

584 system (Caraco et al. 1980).

585

586 Modelling of P species demonstrates that the oxides of Fe, Mn and Al were important for

587 sorption, and these probably exist as very fine oxides phases, as larger particles were

588 generally not detected using SEM. For P_{Total} the best fit model identified Mn_{Total} and organic

589 C as being significant predictors. This is likely because the Fe_{Total} pool will include all the

590 FeS_2, along with various Fe(II) oxide minerals that have low affinities for P. Similarly, the

591 Al_{Total} will include that Al associated with clay. Both Tye *et al*. (2016) and Bortleston (1974)

592 found that when large datasets of sediment P were analysed, Mn_{Total} becomes a significant

593 predictor in models, despite MnO_x generally having a much lower concentration as compared

to FeO_x. This therefore is a limitation on the contribution that MnO_x can make to the binding of P (Bortleston, 1974; Christensen et al., 1997). However, for the $P_{Oxalate}$ model all the oxalate extractable phases measured ($Fe_{Oxalate}$, $Al_{Oxalate}$ and $Mn_{Oxalate}$) were significant predictors in the model. In addition, both $Mn_{Oxalate}$ and $Fe_{Oxalate}$ were highly correlated and

598 were both significant in predicting $NaOH_{Inorganic}$. Whilst $Fe_{Oxalate}$ and $Al_{Oxalate}$ are recognised

599 as surfaces to which P sorbs, the role of $Mn_{Oxalate}$ is less clear as despite its large surface area,

600 its surface chemistry (negative surface charge at near neutral pH; Kawashima et al. 1986) is

601 generally considered less suitable for P sorption than that of FeO_x. However Yao and Millero

602 (1996) found MnO_x to be an important adsorbent of phosphate in seawater whilst Kawasima

603 et al. (1986) suggested that phosphate is sorbed by MnO_x via the presence of divalent cations

604 (Ba^{2+}, Ca^{2+}, Sr^{2+}, Mg^{2+}) or transition metals (Mn^{2+}, Co^{2+}, Ni^{2+}) in aquatic environments.

605 However the strong predictive power of MnO_x found when examined in large datasets is

606 despite the accepted knowledge that FeOOH is likely a far more effective P binding surface.

607 However, particularly in aerobic-anaerobic transition zones of sediments there may be

608 mechanisms that combine the two oxides in the fixation of P. One possibility is that in

609 aerobic-anaerobic transition environments, MnO_x plays a fundamental role in the process

610 through which Fe^{2+} precipitates to form FeOOH or the co-precipitation of Mn/Fe oxy-

611 hydroxides (MnO_x-FeOOH) on which P is later sorbed. This process has been identified in

612 particle analysis from the redox transition zones of ocean waters, where P adsorption forms

613 part of tight element cycling involving Mn-Fe-P (Dellwig et al., 2010). The mechanism

614 involves biogenically produced MnO_x (Tebo et al., 2004) oxidising Fe^{2+} allowing Mn(IV)

615 ions to be replaced by Fe(III) ions. Postma (1985) suggested that the Fe^{3+} produced will most

616 likely precipitate as FeOOH on the surface of the MnO_x particle, followed by immediate

617 adsorption or co-precipitation of P. Thus the suggestion is that one of the reasons MnO_x is

618 identified as being a strong predictive variable in models is because of its link to the pool of

619 FeOOH that is sorbing P. Whilst the $P_{Inorganic}$ was modelled throughout the tidal Thames, no

620 modelling or correlations were found for $P_{Organic.}$

621

One question this study has not been able to answer relates to how long and how much sediment-P remains in temporary storage. Baugh et al. (2013) suggest that during the 20th century the Thames experienced both anthropogenic and natural change in the morphology of the mudflats. In the upper estuary (landward of London Bridge) it is considered that the mudflats have decreased in size due to the tidal channel becoming deeper and wider. However seaward of Barking, the lower estuary has deepened and narrowed leading to a gain in intertidal area. Thus the nature of these mudflats is liable to change over time, with P being stored in different areas of the river as the mudflats develop. When eroded, the material may then be re-deposited within the system. In particular, this is relevant to the deposits in Zones 1 and 2 because any remobilisation and transport downstream is likely to lead to the release of P to the water column as salinity increases in Zones 3 and 4. It is difficult to estimate the age of the samples taken from each individual mudflat because their position and hence deposition environment within the estuary is unique. However, work undertaken looking at the distribution of different pollutants may provide some insights into these questions. For example, Vane et al. (2015) examined Hg through the same core samples as used in this study and in many cores the Hg concentration peaks were found at depths > 30 cm. In their paper they suggested that much of the Hg may have come from the oil and coal burning power stations of London (e.g. Battersea) which closed more than ~40 years ago. Thus it is considered that at least some of the core samples represent an integration of sediment-P processes over many years.

5. Conclusions

The concentration and speciation of P associated with sediments from the foreshore or inter-tidal mud flats of the tidal river Thames were examined. Results demonstrated that both sediment concentration and speciation were largely determined by the position within the

salinity gradient. Whilst representing a temporary store for P, considerable amounts of sediment associated P in zones 1 and 2 remained highly mobile, with the potential of being desorbed if re-suspended and transported to more saline waters. This would lead to potential increases in nutrient status in the outer estuary and contribute to biogeochemical processes. Whilst the behaviour of the inorganic P largely reflects the current state of knowledge with respect to sorption processes, further work exploring the speciation of the organic P species is required, particularly related to the length of time that organic P is stored within mud flat sediments and its utilisation with increasing sediment depth.

Acknowledgements

The authors would like to thank Alex Mortley and the crew of Driftwood III at Port of London Authority (PLA) for providing assistance to CHV in sediment collection. The authors also thank L. Åkesson and all staff at the Environment Agency (Abbey Wood Office) for providing freezers for temporary sample storage. The research was funded by the Land Soil and Coast Directorate, British Geological Survey (BGS). Murray Lark provided advice on model formulation and Simon Chenery on calculating the 'uncertainty propagation' analysis. This paper is published with the permission of the Executive Director, BGS.

6. References

675 Basile-Doelsch, I., Balesdent, J., Rose, J. 2015. Are interactions between organic compounds and nanoscale weathering minerals the key drivers of carbon storage in soils? Environmental Science and Technology, 49, 3997-3998.

Baugh, J., Feates, N., Littlewood, M., Spearman, J. 2013. The fine sediment regime of the Thames estuary – A clearer understanding. Ocean and Coastal management, 79, 10-19.

Beriro, D.J., Vane, C.H., Cave, M.R. and Nathanail, C.P. 2014. Effects of physical sample preparation on the concentrations of polycyclic aromatic hydrocarbons in gasworks contaminated soils. *Chemosphere* 111, 396-404.

Bortleson, G.C. 1974. Phosphorus, iron and manganese distribution in sediment cores of six Winconsin lakes. Limnol Oceanogr: 19, 794-801.

Eyre, B., Balls, P. 1999. A comparative study on nutrient behaviour along the salinity gradient of tropical and temperate estuaries. Estuaries, 22(2A), 313-326.

Caraco, N.F., Cole, J.J., Likens, G.E. 1989. Evidence for sulphate-controlled phosphorus release from sediments of aquatic systems. Nature, 341, 316-318.

Christensen, K.K., Andersen, F.Ø., Jensen, H.S. 1997. Comparison of iron, manganese, and phosphorus retention in freshwater littoral sediment with growth of *Littorella uniflora* and benthic microalgae. Biogeochemistry, 38, 149-171.

Correll, D.L. 1998. The role of phosphate in the eutrophication of receiving waters: A review. Journal of Environmental Quality, 27, 261-266.

Coelho, J.P., Flindt, M.R., Jensen, H.S., Lillebø, A.I., Pardal, M.A. 2004. Phosphorus speciation and availability in intertidal sediments of a temperate estuary: relation to eutrophication and annual P-fluxes. Estuarine, coastal and shelf science, 61, 583-590.

Davidson, K., Gowen, R.J., Harrison, P.J., Flemming, L.E., Hoagland, P., Moschonas, G. 2014. Anthropogenic nutrients and harmful algae in coastal waters. Journal of Environmental Management, 146, 206-216.

Deborde, J., Anschutz, P., Chaillou, G., Etchber, H., Commarieu, M-V., Lecroart, P., Abril, G. 2007. The dynamics of phosphorus in turbid systems: Example of the Gironde estuary (France). Limnology and Oceanography, 52, 862-872.

DEFRA. 2014. Water Framework Directive implementation in England and Wales: new and updated standards to protect the water environment.

Dellwig, O., Leipe, T., März, C., Glockzin, M., Pollehne, F., Schnetger, B., Yakushev, EV., Böttcher, M.E., Brumsack, H-J. 2010. A new particulate Mn-Fe-P shuttle at the redoxcline of anoxic basins. Geochim et Cosmochim Acta, 74: 7100-7115.

Deloffre, J., Verney, R., Lafite, R., Lesueur, P., Lesourd, S., Cundy, A.B. 2007. Sedimentation on intertidal mudflats in the lower part of macrotidal estuaries: Sedimentation rhythms and their preservation. Marine Geology, 241, 19-32.

EA 2014. Water for life and livelihoods – A consultation on the draft update to the river basin management Plan: Part 2: River basin management planning overview and additional information. Environment Agency, Bristol, UK.

EC 2000. Directive 2000/60/EC of the European Parliament and of the Council establishing a framework for the Community action in the field of water policy. Official Journal L 327, p.0001-0073 (22/12/2000)

722 EEC 1991. Council Directive 91/271/EEC concerning urban waste water treatment. .
723
724 Fox, L.E, Sager, S.L., Wofsy, S.C. 1998. The chemical control of soluble phosphorus in the
725 Amazon estuary. Geochimica et Cosmochimica Acta, 50, 783-794.
726
727 Froelich, P.N. 1988 Kinetic control of dissolved phosphate in natural rivers and estuaries: A
728 primer on the phosphate buffer mechanism. Limnoliogy and Oceanography, 33, 649-668.
729
730 Gardolinkski, P.C.F.C., Worsfold, P.J., McKelvie, I.D. 2004. Seawater induced release and
731 transformation of organic and inorganic phosphorus from river sediments. Water Research,
732 38,688-692.
733
734 House, W.A., Denison, F.H. 2000. Factors influencing the measurement of Equilibrium
735 Phosphate Concentrations in river sediments. Water Res: 34, 1187-2000.
736
737 House, W.A., Jickells, T.D., Edwards, A.C., Praska, K.E., Denison, F.H. 1998. Reactions of
738 phosphorus with sediments in fresh and marine waters. Soil Use and Management, 14, 139-
739 146.
740
741 House, W.A., Warwick, M.S. 1999. Interactions of phosphorus with sediments in the River
742 Swale, Yorkshire, UK. Hydrol Process: 13, 1103-1115.
743
744 Inglis, C.C., Allen, F.H. 1957. The regimen of the Thames Estuary as affected by currents,
745 salinities and river flow. Proceedings of the Institution of Civil Engineers, 7, 827-878.
746
747 Jensen, H.S., Mortensen, P.B., Andersen, F.Ø., Rusmussen E., Jensen A. 1995. Phosphorus
748 cycling in a coastal marine sediment, Aarhus Bay, Denmark. Limnology and Oceanography,
749 40(5), 908-917.
750
751 Johnes, P.J., Foy, R., Butterfield, D., Haygarth, P.M. 2007. Land use scenarios for England
752 and Wales: evaluation of management options to support 'good ecological status' in surface
753 waters. Soil Use Manage: 23 (suppl. 1), 176-194.
754
755 Jordan, T.E., Cornwell, J.C., Boynton, W.R., Anderson, J.T. 2008. Changes in phosphorus
756 biogeochemistry along an estuarine salinity gradient: The iron conveyor belt. Limnology and
757 Oceanography, 53, 172-184.
758
759 Kawashima, M., Tainaka, Y., Hori, T., Koyama, M., Takamatsu, T. 1986. Phosphate
760 adsorption onto hydrous manganese (IV) oxide in the presence of divalent cations. Water
761 Res: 20(4), 471-475.
762
763 Kim, J.H., Ludwig, W., Schouten, S., Kerherve, P., Herfort, L., Bonnin, J., Sinninghe Damsté,
764 J.S. 2007. Impact of flood events on the transport of terrestrial organic matter to the ocean: a
765 study of the Tet river (SW France) using the BIT index. Organic Geochemistry, 38, 1593-
766 1606.
767

768 Krom, M.D., Berner, R.A.1980. Adsorption of phosphate in anoxic marine sediments.
769 Limnology and Oceanography, 25, 797-806.
770
771 Lebo, M.E. 1991. Particle-bound phosphorus along an urbanized coastal plian estuary, Marine
772 Chemistry, 34, 225-246.
773
774 Lebo, M.E., Sharp, J.H. 1992. Modelling Phosphorus cycling in a well-mixed coastal Plain
775 estuary. Estuarine, Coastal and Shelf Science, 35, 235-252.
776
777 Littlewood, M., Crossman, M. 2003. Planning for flood risk management in the Thames
778 Estuary. Technical Scoping Report. Environment Agency.
779
780 Lopes dos Santos, R.A and Vane, C.H. 2016. Signatures of tetraether lipids reveal
781 anthropogenic overprinting of natural organic matter in sediments of the Thames estuary,
782 UK. Organic Geochemistry, 93, 68-73.
783
784 Marsh, T.J., Hannaford, J. 2008. The 2007 summer floods in England and Wales – A
785 hydrological appraiosal. Centre for Ecology and Hydrology, UK.
786
787 McKeague, J. A., Day, J. H. 1966. Dithionite and oxalate extractable Fe and Al as aids in
788 differentiating various classes of soils. Canadian Journal of Soil Science, 1966, 46(1): 13-22.
789
790 Mortimer, R.J.G., Krom, M.D., Watson, P.G., Frickers, P.E., Davey, J.T., Clifton, R.J. 1998.
791 Sediment-water exchange of nutrients in the intertidal zone of the Humber estuary, UK.
792 Marine Pollution Bulletin, 37, 261-279.
793
794 Neal, C., Jarvie, H.P., Howarth, S.M., Whithead, P.G., Williams, R.J., Neal, M., Harrow, M.,
795 Wickham, H. 2000. The water quality of the river Kennet: initial observations on a lowland
796 chalk stream impacted by sewage inputs and phosphorus remediation. Science of the Total
797 Environment, 251, 252, 477-4895.
798
799 Neal, C., Neal, M., Leeks, J.L., Old, G., Hill, L., Wickham, H. 2006. Suspended sediment and
800 particulate phosphorus in surface waters of the upper Thames Basin, UK. Journal of
801 Hydrology, 330, 142-154.
802
803 Neal, C., Jarvie, H.P., Williams, R., Love, A., Neal, M., Wickham, H., Harman, S., Armstrong,
804 L. 2010. Declines in phosphorus concentration in the upper River Thames (UK): Links to
805 sewage effluent clean-up and extended end-member mixing analysis. Science of the Total
806 Environment, 408, 1315-1330.
807
808 Pope, N.D., Langston, W.J. 2011. Sources, distribution and temporal variability of trace
809 metals in the Thames Estuary. Hydrobiologia, 672, 49-68.
810

Postma, D. 1985. Concentration of Mn and separation from Fe in sediments – 1. Kinetics and stoichiometry of the eaction between birnessite and dissolved Fe(ii) at 10°C. Geochim et Cosmoschim Acta: 49, 1023-1033.

Powers, S.M., Bruulsema, T.W., Burt, T.P., Chan, N.I., Elser, J.J., Haygarth, P.M., Howden, N.J.K., Jarvie, H.P., Lyu, Y, Peterson, H.M., Sharpley, A.N., Shen, J., Worrall F., Zhang, F. 2016. Long-term accumulation and transport of anthropogenic phosphorus in three river basins. Nature Geoscience 9, 353-356.

Reddy, K.R., Diaz, O.A., Scinto, .L.J, Agani, M. 1995. Phosphorus dynamics in selected wetlands and streams of the lake Okeechobee Basin. Ecol Eng: 5, 183-207.

Reitzel, K., Ahlgren, J., DeBrabandere, H., Waldebäck, M., Gogoll, A., Tranvik, L., Rydin, E. 2007. Degradation rates of organic phosphorus in lake sediment. Biogeochemistry, 82, 15-28.

Ruttenberg, K.C., Sulak, D.J. 2011. Sorption and desorption of dissolved organic phosphorus onto iron (oxyhdr)oxides in seawater. Geochimica et Cosmoschimica Acta, 75, 4095-4112.

Sundareshwar, P.V., Morris, J.T. 1999. Phosphorus sorption characteristics of intertidal marsh sediments along an estuarine salinity gradient. Limnology and Oceanography, 44, 1693-1701.

Thames Water Utilities Ltd. 2011. Technical Appendix C: Water Quality Assessment. LTOA: Phase 2 – Completion of AMP5 Investigations.

Tebo, B.M., Bargar, J.R., Clement, B.G., Dick, G.J., Murray, K.J., Parker, D., Verity, R., Webb, S.M. 2004. Biogenic Manganese Oxides: Properties and mechanisms of formation. Annu Rev Earth Pl Sc: 32, 287-328.

Turner.B.L., Mahieu, N. & Condron, L.M. 2003. The Phosphorus composition of temperate pasture spoils determined by NaOH-EDTA extraction and solution ^{31}P NMR spectroscopy. Organic Geochemistry, 34, 1199-1210.

Tye, A.M., Rawlins, B.G., Rushton J.C., Price R. 2016. Understanding the controls on sediment-P interactions and dynamics along a non-tidal river system in a rural-urban catchment: The River Nene. Applied Geochemistry, 66, 219-233.

Upchurch, J.B., Edzwald, J.K., O'Melia, C.R. 1974. Phosphorus in sediments of Pamlico Estuary. Environmental Science & Technology, 8, 56-58.

Vane, C.H., Beriro, D. and Turner G. 2015. Rise and fall of Mercury (Hg) pollution in sediment cores of the Thames Estuary, London, UK. *Earth and Environmental Science Transactions of the Royal Society of Edinburgh* 105, 4, 285-296

Vane, C.H., Chenery, S.R., Harrison, I., Kim, A.W., Moss-Hayes, V., Jones, D.G. 2011. Chemical Signatures of the Anthropocene in the Clyde Estuary, UK: Sediment hosted Pb, $^{207/206}$Pb, Polyaromatic Hydrocarbon (PAH) and Polychlorinated Biphenyl (PCB) Pollution Records. *Philosophical Transactions of the Royal Society (A)* 369, 1085-1111

Vane, C.H., Harrison; I and Kim, A.W. 2007. Polycyclic aromatic hydrocarbons (PAHs) and polychlorinated biphenyls (PCBs) in sediments from the Mersey Estuary, U.K. *Science of the Total Environment* 374, 112-126.

Vane, C.H., Harrison, I and Kim, A.W. Moss-Hayes, V., Vickers, B.P., Hong, K. 2009. Organic and Metal Contamination in Surface Mangrove Sediments of South China. *Marine Pollution Bulletin*, 58, 14-144.

Vane, C.H., Rawlins. B.G., Kim, A.W., Moss-Hayes, V., Kendrick, C.P., Leng M.J. 2013. Sedimentary transport and fate of polycyclic aromatic hydrocarbons (PAH) from managed burning of moorland vegetation on a blanket peat, South Yorkshire, U.K. *Science of the Total Environment* 449, 81-94.

Wang, Q., Li, Y. 2010. Phosphorus adsorption and desorption behaviour on sediments of different origins. Journal of Soils and Sediments, 10, 1159-1173.

Water Pollution Research Laboratory, 1964. Effects of polluting discharges on the Thames Estuary. The Reports of the Thames Survey Committee and the Water Pollution Research Laboratory. Water Pollution Research Technical Paper 11. HMSO.

Worsfield, P.J., Monbet, P., Tappin, A.D., Fitzsimmons, M.F., Stiles, D.A., McKelvie, I.D. 2008. Characterisation and quantification of organic phosphorus and organic nitrogen components in aquatic systems. A Review. Analytica Chimica Acta, 624, 37-58.

Yao, W., Millero, F.J. 1996. Adsorption of phosphate on manganese dioxide in seawater. Environmental Science and Technology, 30, 536-541.

Zhang, J.Z., Huang, X.L. 2011. Effects of temperature and salinity on phosphate sorption on marine sediments. Environmental Science and Technology, 45, 6831-6837.

Zwolsman, J.J.G. 1994.Seasonal variability and biogeochemistry of phosphorus in the Scheldt Estuary, south-west Netherlands. Estuarine, Coastal and Shelf Science, 39, 227-248.

Table 1: Output from observed v predicted regression model for P_{Total} sediments

Coefficient	Estimate	Std Error	t-value
Intercept	1.1946	0.1532	7.795
Log Mn (mg kg^{-1})	0.7457	0.0582	12.811
TOC (%)	0.0626	0.0079	7.842
Salinity (ppt)	-0.0061	0.0011	-5.240

Residual standard error: 0.1585 on 249 degrees of freedom
Multiple R-squared: 0.80, Adjusted R-squared: 0.80
F-statistic: 344 on 3 and 249 DF, *p*-value: < 2.2e-16

Table 2: Output for observed v predicted regression model for $P_{Oxalate}$ in t sediments

Coefficient	Estimate	Std Error	t-value	
Intercept	-0.339	0.273	-1.240	
Log Mn (mg kg^{-1})	0.437	0.058	7.495	<
Log Fe (mg kg^{-1})	0.381	0.057	6.592	<
Log Al (mg kg^{-1})	0.321	0.075	4.239	<
Salinity (ppt)	-0.011	0.001	-8.582	<

Residual standard error: 0.208 on 279 degrees of freedom
Multiple R-squared: 0.80, Adjusted R-squared: 0.80
F-statistic: 287.5 on 4 and 279 DF, *p*-value: < 2.2e-16

Table 3: Outputs for observed v predicted regression model for $P_{Inorganic}$ ext NaOH for the Thames sediments.

Coefficient	Estimate	Std Error	t-value
Intercept	0.4880	0.1915	2.548
Log $Mn_{Oxalate}$ (mg kg^{-1})	0.5048	0.0636	7.928
Log $Fe_{Oxalate}$ (mg kg^{-1})	0.3231	0.0640	5.042
Salinity	-0.0130	0.0014	-9.273

Residual standard error: 0.2123 on 260 degrees of freedom
Multiple R-squared: 0.767, Adjusted R-squared: 0.7643 F-statistic: 285.3 on 3 and 260 DF, p-value: < 2.2e-16

Figure 1: Map of sampling sites for core samples taken from the tidal River Thames

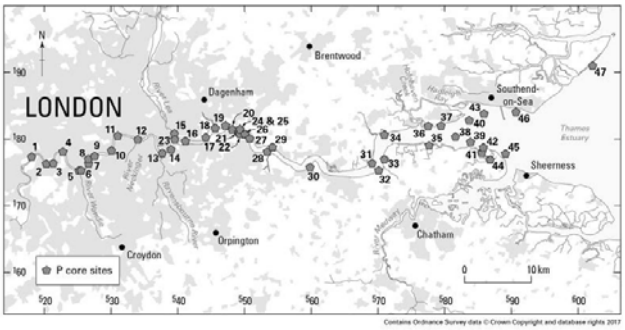

Figure 2: Map of sampling sites for grab samples (0-3cm) taken from the tidal River Thames

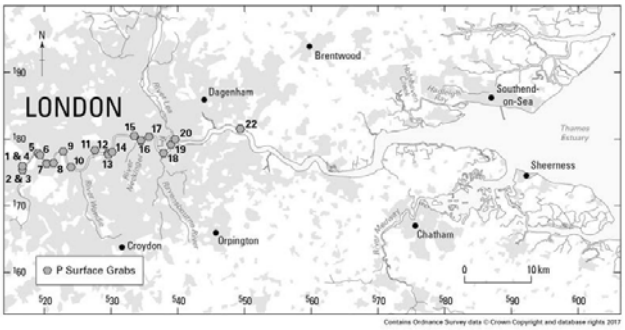

Figure 3: Characteristics of sediment geochemistry. Graphs (a) and (b) show the relationship between the mean concentration of total Al and Si in the cores with distance from Teddington Lock respectively. In graph C the relationship between total Al and Rb in the 10 cm sediment core sections from all samples are shown (n=260) demonstrating that the sediment is largely derived from one well mixed source throughout the estuary.

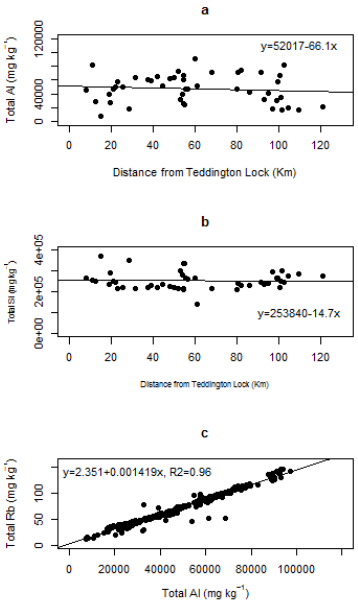

Figure 4: Graph showing (a) sediment depth of cores (cm), (b) a typical salinity (ppt) profile for the tidal Thames taken from Pope & Langston (2011) and (c) mean P_{Total} concentrations (mg kg^{-1}) for the cores. All are plotted against the distance of the sample from Teddington Lock.

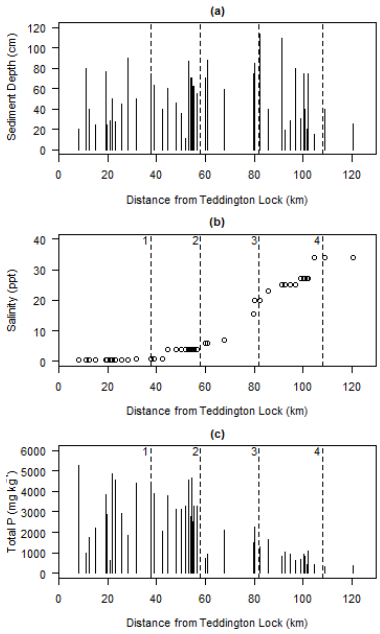

Figure 5: Box and Whisker plots showing the variation in concentration of P_{Total} in 10 cm core sections of cores taken from each of the four estuary zones designated by Littlewood and Crossman (2003) and the grab samples (0-3cm) taken in Zones 1 and 2. The zones are shown in order of distance from Teddington Lock.

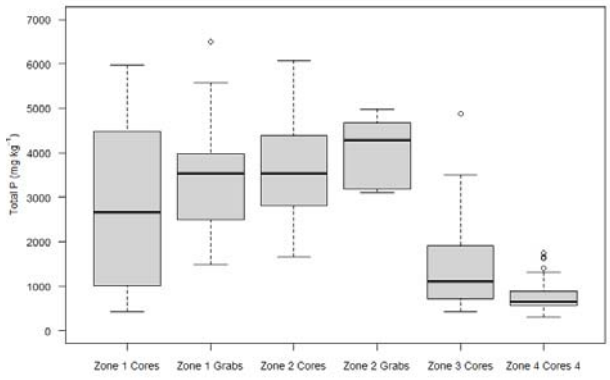

Figure 6: Correlations of P_{Total} with other elements associated with the sequestration of Phosphorus

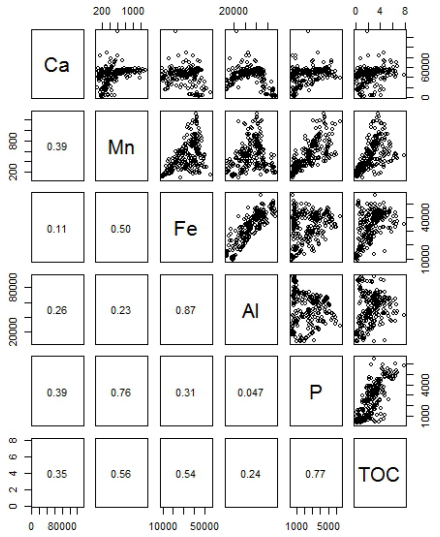

Figure 7: BSEM images taken at 20 kV. Figure 7A (Core 35, depth 10-20 cm) illustrates the ubiquity of FeS_2 (pyrite) in the sediment as the widespread, locally clustered, bright areas. Figure 7B (Core 29, 40-50 cm) shows clustered, framboidal, pyrite.

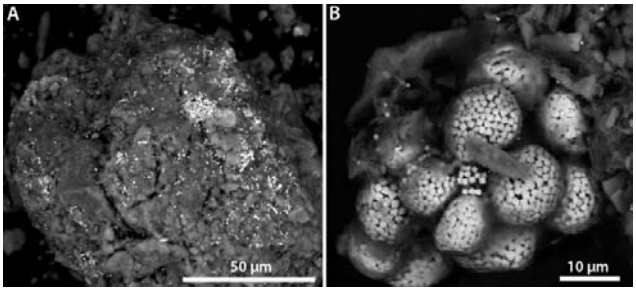

Figure 8: Observed v Predicted regression model for Log P_{Total} for muddy flat sediments in the tidal river Thames. Results of the regression model can be seen in Table 1.

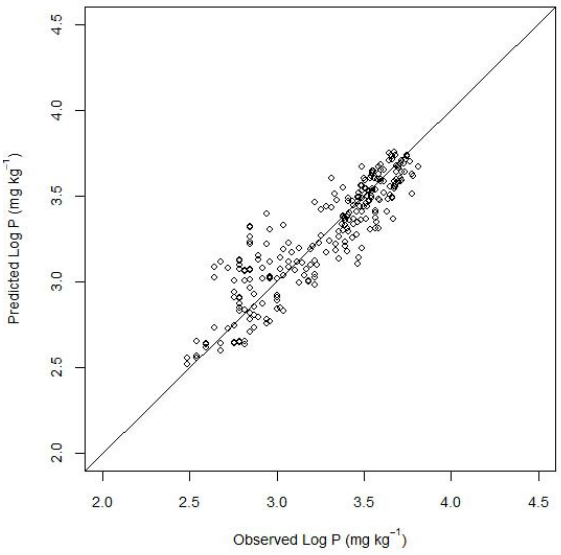

Fig 9: The relationships between oxalate extractable and total concentrations for (a) Fe, (b) Al and (c) and Mn which act as binding surfaces for P in river sediments. In Figures (a) and (b) closed symbols represent samples from Zone 1 and 2 whilst open symbols represent samples from Zones 3 and 4.

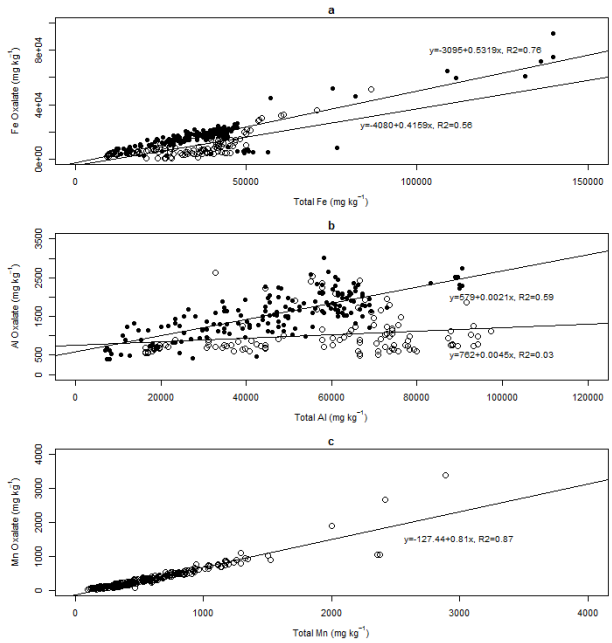

Fig 10: The relationship between P_{Total} and $P_{Oxalate}$ in foreshore sediments of the River Thames.

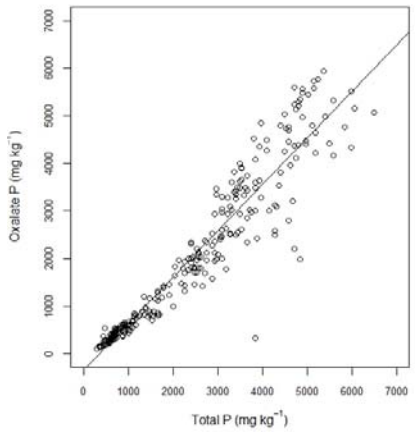

Fig 11: Boxplot showings the range of values of P_{Total}:$P_{Oxalate}$ from Zones 1 and 2 and those from Zones 3 & 4 demonstrating the change in this relationship with increasing salinity.

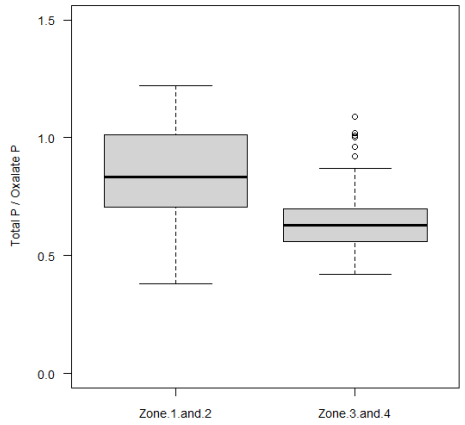

Figure 12: Correlation relationships shown between oxalate extractable P, Al, Mn and Fe in Thames sediments

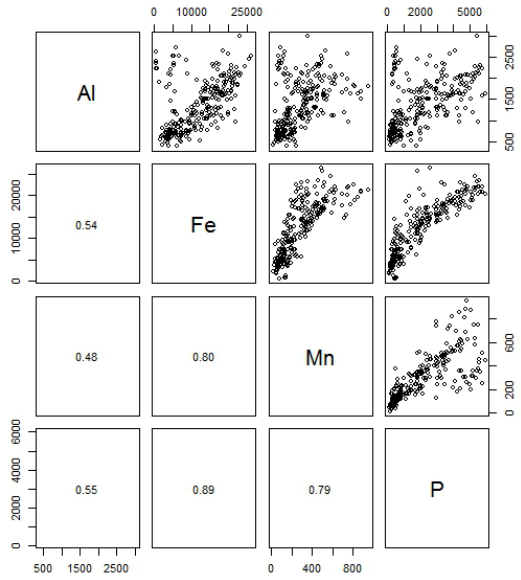

Figure 13: Box and whisker plots to show the range of the Degree of Phosphorus saturation (DSP) in Thames sediments from the four sediment zones and grab samples taken from Zones 1 and 2.

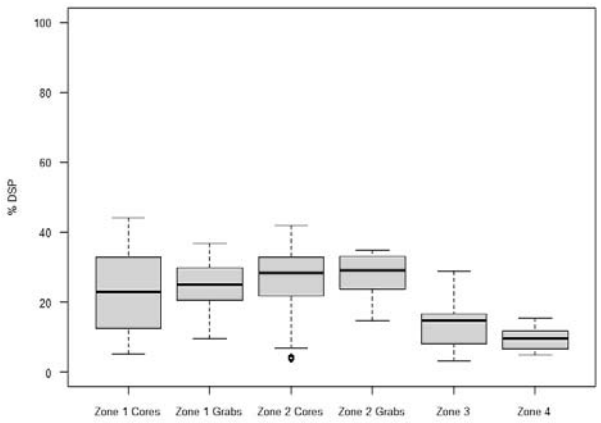

Figure 14: Observed v predicted for model describing the relationships of Log $P_{Oxalate}$ to binding phases in Thames foreshore sediments. Results of the regression model can be seen in Table 2.

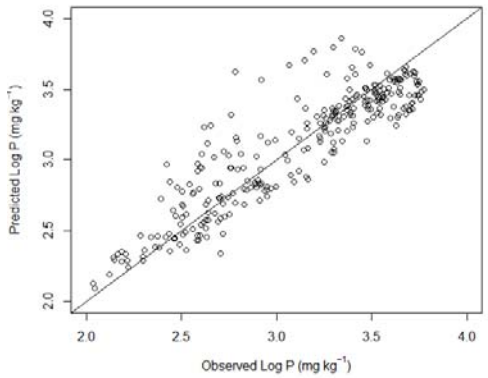

Figure 15: The relationship between concentrations of NaOH extractable $P_{Inorganic}$ and $P_{Organic}$ in three depth segments (0-10 cm, 30-40 cm and 50-60 cm) in cores with distance from Teddington Lock. Cores in Zone 1 are those numbered 1 - 12, in Zone 2 core number 13 - 27, in Zone 3 cores are numbered 28 - 33 and Zone 4 cores are numbered 34 – 47.

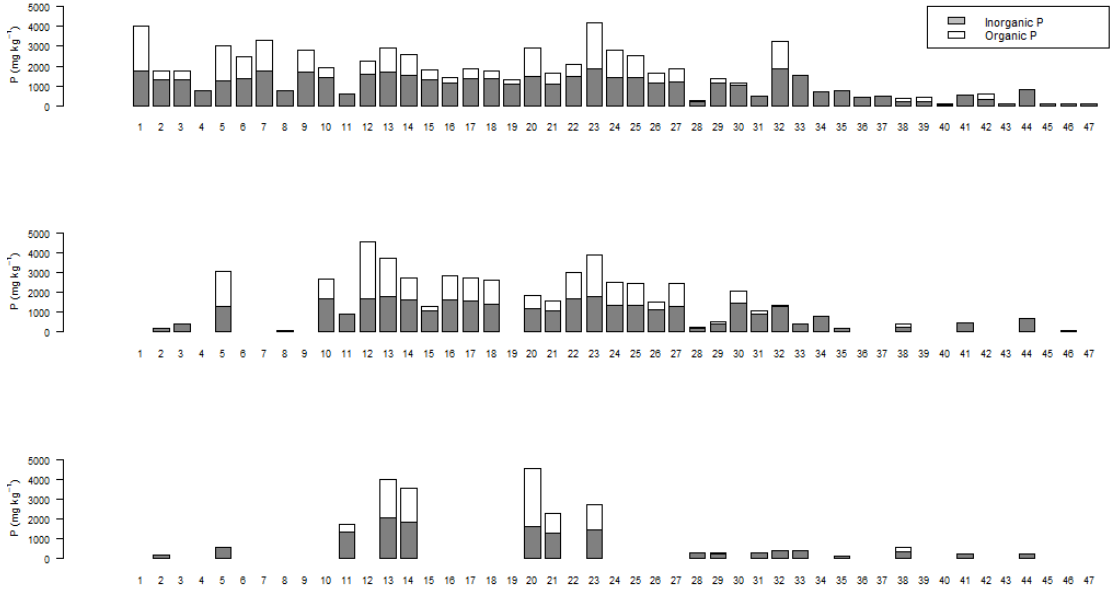

Figure 16: Observed v predicted for model describing the relationships of Log $P_{Inorganic}$ extracted using NaOH to binding phases in Thames foreshore sediments. Results of the regression model can be seen in Table 3. Solid line is the 1:1 line.

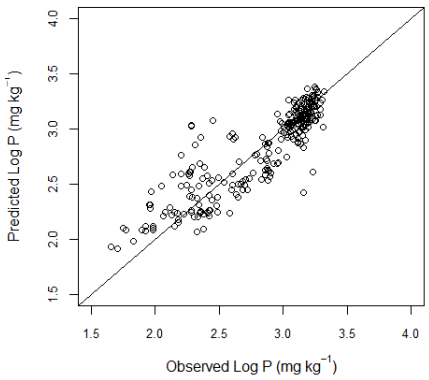

Figure 17: Conceptual model of sediment P behaviour in the Thames estuary based on data from this study on inter-tidal mud deposits. The sediment zones of Littlewood and Crossman (2003) are used with salinity values from Pope and Langston (2011).